Chemosphere 359 (2024) 142229

Contents lists available at ScienceDirect

Chemosphere

journal homepage: www.elsevier.com/locate/chemosphere

The effectiveness and feasibility of ball-milled powdered activated carbon (BPAC) for removal of organic pesticides in conventional drinking water treatment process

Wei Li [a,*], Congjian Dong [a], Zijing Hao [a], Xinyi Wu [a], Donghai Ding [b], Jinming Duan [c,**]

[a] Key Laboratory of Northwest Water Resources, Environment and Ecology, MOE, Xi'an University of Architecture and Technology, 13 Yanta Road, Xi'an, 710055, China
[b] College of Materials Science and Engineering, Xi'an University of Architecture and Technology, 13 Yanta Road, Xi'an, 710055, China
[c] Centre for Water Management and Reuse, UniSA STEM, University of South Australia, Mawson Lakes Campus, SA, 5095, Australia

HIGHLIGHTS

- Ball-milled PAC (BPAC) increase greatly pesticide adsorption kinetics.
- Diffusional adsorption from bulk to PAC surface could be a predominant mechanism.
- Adsorption is driven by enthalpy or entropy depending on pesticide hydrophobicity.
- BPAC of 1 μm led to pesticide-loaded particle penetration through the filter media.
- BPAC of 6 μm effectively removes pesticides while controlling particle penetration.

GRAPHICAL ABSTRACT

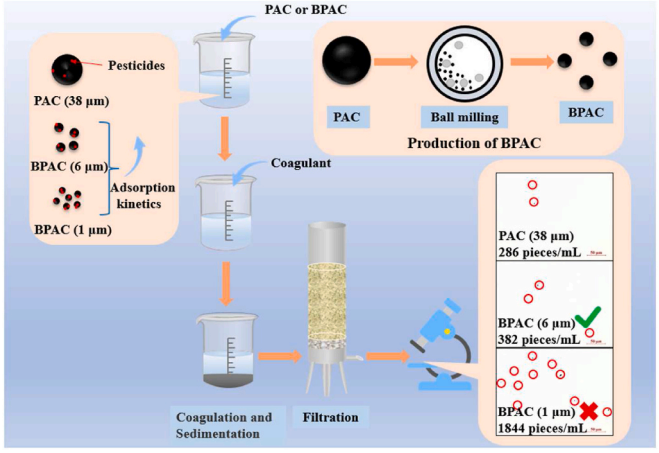

ARTICLE INFO

Handling Editor: Yongmei Li

Keywords:
Powdered activated carbon
Ball-milled PAC
Pesticides
Conventional drinking water treatment

ABSTRACT

In the conventional drinking water treatment process (CDWTP), powdered activated carbon (PAC) is commonly used for removing organic pesticides, or other organic contaminants. However, the hydraulic retention time (HRT) in CDWTP is insufficient for fulfilling PAC adsorption equilibrium to realize its full capacity. This study examined the adsorption kinetics, adsorption thermal dynamics, and removal efficiency for six organic pesticides using the ball-milled PAC (BPAC) with varying particle sizes in CDWTP. Based on the experiments with the pesticides of atrazine, diazinon, dimethoate, fenitrothion, isoproturon and thiometon, the results indicated that as the particle size reduced from around 38 μm for the commercial PAC to 1 μm for the BPAC, the adsorption rates for hydrophobic pesticides increased up to twentyfold. Diffusional adsorption from the bulk solution to the

* Corresponding author.
** Corresponding author.
E-mail addresses: liwei@xauat.edu.cn (W. Li), Jinming.Duan@unisa.edu.au (J. Duan).

https://doi.org/10.1016/j.chemosphere.2024.142229
Received 13 February 2024; Received in revised form 19 April 2024; Accepted 1 May 2024
Available online 7 May 2024

external PAC surface is the most likely predominant mechanism. This could allow a sufficient pesticides' adsorption within the limited HRT and to achieve a great depth removal of these toxic compounds. However, the addition of BPAC with a diameter of 1 μm was observed to significantly increase residual particles in treated water after the conventional treatment process. With a further systematic evaluation of both adsorption rate and particle penetration, a particle size of around 6 μm BPAC was considered a practical compromise between the adsorption rate and particle penetration for real application. Results from five surface waters of different water quality indicated that, compared to commercial PAC, application of 6 μm BPAC could achieve up to a 75% reduction in adsorbent dosage while maintaining around the same pesticide removal efficiencies. Additionally, thermodynamic analyses suggest that adsorption of these pesticides could be enthalpically or entropically driven depending on the degree of pesticide hydrophobicity.

1. Introduction

Chemical pesticides are extensively used in modern agriculture to bolster productivity and ensure food security in the face of population growth (Nicolopoulou-Stamati et al., 2016; Tudi et al., 2021). According to the Statista Research Department, global agricultural pesticide consumption exhibited a predominantly steady increase, rising from 2.18 million metric tons in 2000 to 3.54 million metric tons in 2021 (Statista Research Department, 2023). Despite the efforts for efficient usage of pesticides, it is estimated that only 0.1% of pesticides applied for pest control reach the target pests, leaving most of the chemicals remaining on plant surfaces or entering the environments, including the soil and atmosphere (Khan, 2016; Pimentel, 1995). The pesticides could be transported by runoff into aquatic environments, leading to varying degrees of contaminations in natural waters.

The concentration of pesticides in surface waters and groundwater may range from dozens of nanograms to several micrograms per liter (Gilliom, 2007; Meffe and de Bustamante, 2014). In regions where agricultural and urban areas are subjected to pesticide application, their concentrations in the water bodies may rise to dozens of micrograms per liter or even higher (de Souza et al., 2020; Meftaul et al., 2020). Toxicological and epidemiological studies have suggested that long-term exposure to low levels of pesticide (primarily through diet or drinking water) could lead to adverse effects on humans, including an elevated risk of cancer and potential disruptions to metabolic functioning, as well as adverse impacts on the reproductive, immune, endocrine, and nervous systems (Mostafalou and Abdollahi, 2017; Naughton and Terry Jr, 2018; Richardson et al., 2019). To protect the public health, governments worldwide have implemented the residual limits for pesticides in drinking water. For example, 31 pesticides are listed in the World Health Organization (WHO) guidelines for drinking water quality (fourth edition) based on health safety factors (WHO, 2011). Therefore, efficient removal of pesticides from source water is considered crucial for safe water quality.

Conventional process of coagulation/flocculation, sedimentation and filtration (CSF) has been found ineffective in removing organic pesticides from water, likely due to the small molecular size and high water solubility of the pollutants (Alexander et al., 2012; Li et al., 2018). In recently years, various advanced treatment technologies, include biological methods (such as biofiltration), chemical oxidation techniques (e.g., ozonation, advanced oxidation processes (AOPs)) and physical methods (e.g., activated carbon adsorption, membrane filtration), have been developed to improve the removal of pesticides. Biological methods, such as biofiltration, may provide an environmentally friendly and cost-effective approach. However, it seems that the slow reaction kinetics hindered its wide application in water treatment plants (Ahmed et al., 2021; Desisa et al., 2022). Chemical oxidation methods especially AOPs have been extensively studied in laboratory scale for pesticides degradation and even mineralization. Although pesticides could be decomposed by AOPs, the degradation byproducts may exhibit much higher toxicity than the parent compounds (Ahmed et al., 2021; Li et al., 2019). Furthermore, mineralization of these pesticides typically requires a large amount of energy input and a very long reaction time, making it impractical (Li et al., 2019). Membrane filtration, mainly including nanofiltration (NF) and reverse osmosis (RO), is effective in removing hydrophobic pesticides but demands a considerable initial investment, substantial energy input and is prone to membrane fouling and deterioration, making it financially unaffordable for some of the developing countries (Ahmed et al., 2021; Brovini et al., 2023). In comparison, powdered activated carbon (PAC) has been an economical and effective option for removing pesticides and widely used in drinking water treatment (Campinas et al., 2021; Li et al., 2016; Matsushita et al., 2018). However, the hydraulic retention time (HRT) in the conventional flocculation basin is substantially shorter than the time required for PAC adsorption equilibrium (Al-Asad et al., 2022; Najm, 1996). This leads to a low utilization efficiency of activated carbon, significantly reducing the adsorption capacity of PAC, and consequently increasing water treatment costs.

It has been reported that the ball-milled PAC (BPAC) with superfine particles (submicron) were effective in removing natural organic matters (NOM), odor and taste compounds, as well as synthetic organic contaminants (SOCs) from water in recent studies (Bonvin et al., 2016; Matsui et al., 2015; Nakayama et al., 2020). However, the application of extremely fine PAC particles could possibly result in a penetration of micropollutant-loaded PAC particles through conventional CSF processes, particularly the filter media bed, entering into drinking water supplies (Nakazawa et al., 2018). This would thereby pose potential risks to consumers due to micropollutant desorption within the digestive system (Siri et al., 2021). Therefore, the application of BPAC in water treatment would require consideration of both effective removal of the target contaminants and the adsorbent PAC. In the present study, six pesticides (atrazine, diazinon, dimethoate, fenitrothion, isoproturon and thiometon) were selected for a systematic examination of the adsorption kinetics and thermal dynamics, as well as the removal efficiencies with different particle sizes of BPAC, derived from a commercial PAC. At the same time, with an establishment of laboratory testing protocol, the residual fine PAC penetration was also examined under all the particle size conditions. The optimal PAC particle size was subsequently established through a comprehensive evaluation of both the residual pesticide concentration and PAC particles in the filtrate following conventional CSF treatment. Finally, a feasibility experimental demonstration of the optimal BPAC for five different surface waters was conducted for pesticide removal within the CSF processes.

2. Materials and methods

2.1. Chemicals and materials

Atrazine (98.8% purity), diazinon (99.5% purity), dimethoate (99.1% purity), fenitrothion (99.1% purity), isoproturon (99.1% purity) and thiometon (99% purity) were purchased from AccuStandard Inc. (New Haven, CT, USA). Table S1 provides their molecular structure, molecular weight (MW), water solubility and octanol-water partition coefficient (log*K*ow). Aluminum sulfate ($Al_2(SO_4)_3 \bullet 18H_2O$, analytical grade) was purchased from Sinopharm Chemical Reagent Co. Ltd. (Shanghai, China). A commercial coal-based PAC was supplied by the Bailuyuan drinking water treatment plant in Xi'an City, China. The PAC was dried in an oven at 150 °C for 1 h and stored in a desiccator before

use. Ultrapure water was produced by an Elga Purelab Ultra Analytic system (Bucks, UK).

BPAC was produced from commercial PAC using a planetary ball milling machine (XQM-2L, Nanjing Kexi Experimental Instrument Research Institute, China) with 0.3–8 mm yttrium-stabilized zirconia (YSZ) ceramic beads. Milling was carried out for 6 h with recirculated milling in ultrapure water without dispersant, and the ball-milled PACs were stored in slurry form at a concentration of 10 g/L and kept at 4 °C. Before use, the slurries were stirred and subjected to ultrasonication to ensure a uniform dispersion of carbon.

2.2. Sampling

The raw water sample free of target pesticides was obtained from the Jinpen Reservoir, a valley-dammed reservoir and the primary drinking water source in Xi'an City, China. The water samples were filtered through Whatman 2.7 μm GF/D glass microfiber filters (diameter 47 mm, pore size 2.7 μm) and stored in amber glass bottles in a refrigerator at 4 °C until use. Additionally, four more surface water samples were collected from the Feng River, the Wei River, the Shibianyu Reservoir and the Hancheng Lake around the region of Xi'an, China. The major water quality parameters of these water samples are listed in Table S2 and Fig. S1.

2.3. Experimental procedures

2.3.1. Adsorption experiments

The adsorption process of the target pesticides onto the PAC or BPAC was conducted through batch experiments. In adsorption kinetic experiments, 10 mg/L of PAC or BPAC was transferred into 125-mL glass Erlenmeyer flasks containing 100 mL of raw water from the Jinpen Reservoir with an initial individual pesticide concentration of 10 μg/L. A magnetic stirrer operating at a constant speed of 200 rpm maintained uniform dispersion of the reacting solution, and an incubator controlled the solution temperature at 25 ± 1 °C. At designated time intervals, 5 mL aqueous samples were withdrawn using a glass syringe, filtered through a 0.45 μm glass membrane filter (GD/X Syringe Filters, Whatman), and then mixed with 30% methanol (v/v) in the filtrate to avoid the loss of analytes due to the adsorption effect (Li et al., 2015). Subsequently, the mixture was transferred to a glass vial after filtration by a 0.2 μm pore size Acrodisc® hydrophilic polypropylene (GHP) syringe filter (Pall Gelman Laboratory, Ann Arbor, MI, USA) for the measurement of residual pesticides.

In the subsequent adsorption isotherm experiments, all operational procedures remained the same to those described above, with the exception of varying adsorbent dosage (5–20 mg/L) and maintaining continuous stirring for 12 h for achieving the adsorption equilibrium. Additionally, the thermodynamic experiments involved controlling reaction temperatures (15, 20, 25, and 30 ± 1 °C) using an incubator, for purpose of the establishment of thermal dynamic parameters.

The amounts of pesticides adsorbed onto commercial PAC or BPAC at time t (q_t; μg/mg) was calculated by Eq. (1):

$$q_t = \frac{(C_0 - C_t)V}{m} \quad (1)$$

where.

q_t (μg/mg) is the adsorbent loading at time t; C_0 (μg/L) and C_t (μg/L) are the initial and residual concentration of pesticides at time t, respectively; m (mg) is the mass of adsorbent, and V (L) is the volume of the solution.

2.3.2. Jar test procedures

Bench-scale jar test experiments were performed using a jar test apparatus (JJ-4C, Suzhou Well Scientific Ltd, China) where the stirring intensity (rpm) and time were preset. It consists of six flat-paddle impellers and standard 2-liter square beakers. To simulate the PAC assisted CSF treatment process, the following procedures were employed: a dose of PAC or BPAC (5, 10, 15, 20, 30, 50, 60 mg/L) was added to the beaker containing 1 L of surface water pre-spiked with individual pesticide concentration of 10 μg/L and maintained under 200-rpm for 6 min (contact time of about 6 min in an actual drinking water treatment plant). Following this, 120 μM alum coagulant was added, followed immediately by 250-rpm rapid mixing for 1 min, then 30-rpm slow mixing for 15 min, and a quiescent settling for 30 min. At the end of sedimentation, the supernatant from each jar was gently withdrawn from approximately 2 cm below the water surface using a wide mouth pipet and analyzed for settled turbidity; a 5 mL water sample was taken and treated using the same sample pretreatment procedures described above (see section 2.3.1) for the measurement of residual pesticides. Afterward, the settled water was filtered using a lab-scale sand filter (the schematic diagram is illustrated in Supplementary Fig. S2) to measure both filtered turbidity and the quantity of PAC particles that permeated the filter.

All the experiments were conducted in triplicate, and average values and standard deviations were reported.

2.4. Analytical methods

The particle size distribution of PAC and BPAC was determined using a laser particle size analyzer (Sync, Microtrac, USA). The BET (Brunauer-Emmett-Teller) surface area, pore volume and pore size distribution were characterized with nitrogen adsorption/desorption analysis measurements (ASAP 2460, Micromeritics Inc., USA) at 77.4 K. The turbidity (Nephelometric turbidity units, NTU) of water samples was measured using a turbidity meter (2100P, Hach, USA). The Fourier transform infrared (FTIR) spectra of PAC and BPAC (4000 - 500 cm^{-1}) was recorded using a Nicolet 6700 FT-IR spectrophotometer (Thermo Scientific, USA).

The enumeration of the PAC particles in the sand filtered effluent followed a previously established method with minor modifications (Nakazawa et al., 2018). In brief, 100 mL of the filtered water was filtered through a GHP membrane with 47 mm diameter and 0.2 μm pore size (Pall Gelman Laboratory, Ann Arbor, MI, USA) supported by a 47 mm glass filter holder (Jinteng experiment equipment company, Tianjin, China). After that, a digital microscope (Nikon 50i, Tokyo, Japan) operating at 400 × magnification was employed to capture color digital photomicrographs at nine pre-determined observation zones (microscope view area: 230× 310 μm) per filter (Fig. S3). The obtained photomicrographs were analyzed using the Nikon NIS-Elements™ software provided with the microscope.

The point of zero charge pH (pH_{PZC}) of PAC and BPAC was measured using the pH drift method proposed by Günther Müller et al. (1985) (Müller et al., 1985). Briefly, 20 mL of 0.01 M NaCl was added to a series of Erlenmeyer flasks. The pH values were initially set to a range of 3–11 by adding 0.1 M HCl or 0.1 M NaOH solution. The initial pH values of the solutions were measured and recorded as pH_I. Once the pH_I reached the constant value, PAC or BPAC (50 mg) was introduced into each Erlenmeyer flask and shaken for 48 h at 25 °C. Subsequently, the final pH of the solutions was measured and recorded as pH_F. The pH_{PZC} was determined as the point where the curve of ΔpH (pH_F - pH_I) versus pH_I intersects the line equal to zero, or $pH_F = pH_I$.

The quantitative analysis of six pesticides was performed using ultra-performance liquid chromatography-electrospray tandem mass spectrometry (UPLC-ESI-MS/MS, Waters, Milford, MA, USA) with an ACQUITY™ UPLC HSS T3 separation column (2.1 × 100 mm, 1.8 μm particle size, Waters) as reported in our previous work (Li et al., 2015). Briefly, the separation started with 10% MeOH for 2 min, followed by an increase to 100% within 7 min, which was then maintained for 2 min. Finally, the ratio of MeOH was reduced back to 10% and maintained for 3 min for equilibrium before the next injection. The column temperature was maintained at 35 °C and the injection volume was 10 μL. The

UPLC-ESI-MS/MS was operated in positive electrospray ionization (ESI+) mode with a desolvation temperature set at 350 °C and a source temperature at 110 °C. The capillary voltage was set at 3.5 kV, with nitrogen (99.999%) as the desolvation and cone gas at flow rates of 600 L/h and 30 L/h, respectively. The collision gas was argon (99.999%) at a flow rate of 0.12 mL/min. Data acquisition and processing were performed using Masslynx 4.1 software (Waters Corporation). The retention time (RT), cone voltage (CV), transition ions, and collision energy (CE), limits of detection (LODs) and limits of quantification (LOQs) for the individual pesticides are listed in Table S1.

2.5. Adsorption analysis

The pseudo-second order model and Langmuir isotherm model have been shown to give the best fitting for the PAC and BPAC adsorption data of the pesticides after trials of several relevant models (see supplementary materials Text S1, S2 and Tables S3 and S4). Consequently, these two models were selected to characterize the PAC adsorption kinetics and adsorption isotherms of pesticides, respectively.

2.5.1. Pseudo-second order kinetics

The pseudo-second order kinetics can be expressed as Eq. (2),

$$\frac{dq_t}{dt} = k_2(q_e - q_t)^2 \tag{2}$$

which is commonly used in the linearized form developed by Ho and McKay (1999) (Ho and McKay, 1999):

$$\frac{t}{q_t} = \left(\frac{1}{q_e}\right)t + \frac{1}{k_2 q_e^2} \tag{3}$$

where.

q_e (μg/mg) is the adsorbed pesticide amount per unit of the adsorbent at equilibrium; k_2 (mg/(μg min)) is the pseudo-second order rate constant.

In accordance with Simonin (2016) (Simonin, 2016), by defining $k^* = k_2 q_e$, Eq. (3) may be rewritten as,

$$q_t = q_e \frac{k^* t}{1 + k^* t} \tag{4}$$

or

$$F(t) = \frac{k^* t}{1 + k^* t} \tag{5}$$

Eq. (5) reveals that the change in dimensionless solid-phase concentration is proportional to the t, indicating that the value of k^* (min^{-1}) really reflects the kinetic performance (Wu et al., 2009). This parameter, defined as the rate index, is commonly used to assess adsorption rates (Simonin, 2016; Wu et al., 2009).

2.5.2. Langmuir isotherm

The Langmuir adsorption isotherm can be expressed by Eq. (6) (Ghosal and Gupta, 2017),

$$q_e = \frac{q_{max} K_L C_e}{1 + K_L C_e} \tag{6}$$

where.

C_e (μg/L) is the concentrations of pesticides in solution; q_{max} (μg/mg) is the maximum pesticide adsorption capacity and K_L (L/μg) refers to the Langmuir isotherm constant, which is related to the binding energy or affinity parameter of the adsorption system (Ghosal and Gupta, 2017).

2.5.3. Adsorption thermodynamics

To investigate adsorption mechanisms, adsorption thermodynamics were analyzed using the thermodynamic equilibrium coefficients obtained at different temperatures. The free energy change in an adsorption process can be typically related to the equilibrium constant (K_C) by the Gibbs fundamental equation, as expressed by Eq. (7) (Ghosal and Gupta, 2017),

$$\triangle G^o = -RT \ln K_C \tag{7}$$

in which ΔG° (J/mol) is the standard free energy change, R (8.314 J/(mol K)) the universal gas constant, T (K) is the absolute temperature. K_C is the thermodynamic equilibrium constant, which could be calculated from the equilibrium constant of the Langmuir equation as $K_C = 10^6 K_L$ (Tran et al., 2017). The relationship of ΔG° to enthalpy change (ΔH°, kJ/mol) and entropy change (ΔS°, J/(mol K)) of adsorption can be expressed as

$$\triangle G^o = \triangle H^o - T\triangle S^o \tag{8}$$

Substituting Eq. (8) into Eq. (7) gives van't Hoff plot:

$$\ln K_C = -\frac{\triangle H^o}{RT} + \frac{\triangle S^o}{R} \tag{9}$$

The plot of $\ln K_C$ against 1/T theoretically produces a straight line, enabling the calculation of ΔH° and ΔS° from the respective slope and intercept of Eq. (9).

2.6. Statistical analysis

The experimental data were analyzed using the Statistical Package for the Social Sciences (SPSS) software version 26 (SPSS Inc, Chicago, Illinois, USA). The correlation analysis was used to analyze the significant relationship between the particle size of BPAC and adsorption parameters (K_L and q_{max}), with results reported at a 95% confidence interval, using an α-value of 0.05. If the p-value obtained from the test is less than α, $p < 0.05$, the difference is considered statistically significant; if the $p > 0.05$, it suggests no statistical significance (Zhang et al., 2021).

3. Results and discussion

3.1. Physic-chemical properties of PAC and BPAC

Table 1 depicts the physic-chemical properties of the activated carbon before and after ball milling, including the particles' median diameter (D_{50}), Brunauer-Emmett-Teller (BET) specific surface area, total pore volume (V_T), pore size distribution and pH_{PZC}. After ball milling, the D_{50} of PAC particles decreased from 37.8 μm to 1.1 μm. For convenience of discussions, these PAC particles are labeled as PAC-38, PAC-25, PAC-12, PAC-6, and PAC-1 based on their respective D_{50} values. Interestingly, as the particle size decreasing, the BET specific surface area of the PAC decreases noticeably from 1367 m^2/g for commercial PAC-38 to 1214 m^2/g for PAC-1. This observation contrasts with the trend normally observed with solid particles, where BET specific surface areas will increase as particles break down into smaller sizes. For porous PAC, apart from outer specific surface area, the change in the inner pore surface area could also impact the BET surface area. Although the BET surface analysis couldn't discern between the internal pore surface and the external surface of the PAC particles, it is obvious that the external surface of PAC particles will increase with the breakup of the PAC particles following the milling process. As indicated in Table 1, with the decrease in particle size from approximately 38 μm–1 μm, the micropore (pore width <2 nm) size distribution decreased from 0.42 cm^3/g to 0.34 cm^3/g, while mesopore (pore width of 2–50 nm) size distribution increases from 0.38 cm^3/g to 0.45 cm^3/g. It appears that the pores survived from or produced by the milling process are slightly larger than those before milling, suggesting that milling may crush some of the very small pores of PAC, resulting in a slight reduction in BET specific surface area.

In addition, it seems that the ball milling has a visible impact on the

Table 1
The median particle diameter, Brunauer-Emmett-Teller (BET) surface area, average pore diameter (D_{Pore}), total pore volume (V_{Total}) and pore size distribution, as well as the pH at the point of zero charge (pH_{PZC}) of both PAC and BPACs.

Lable	Diameter (μm)	BET (m^2/g)	D_{Pore} (nm)	V_{Total} (cm^3/g)	Pore size distribution (cm^3/g)			pH_{PZC}
					Micropore (<2 nm)	Mesopore (2–50 nm)	Macropore (>50 nm)	
PAC-38	37.8	1367	2.85	0.83	0.42	0.38	0.03	9.86
PAC-25	25.2	1343	2.87	0.82	0.40	0.38	0.04	8.92
PAC-12	12.4	1289	2.96	0.84	0.36	0.44	0.04	7.85
PAC-6	5.8	1266	2.99	0.86	0.37	0.43	0.06	7.43
PAC-1	1.1	1214	3.16	0.84	0.34	0.45	0.05	7.26

chemical properties of the PAC. After the ball milling, the pH_{PZC} values of the PAC particles showed a gradual decline, reducing from 9.86 for the parent PAC to 7.26 for PAC-1. As shown in Fig. S4, the FTIR spectrum of PAC and BPACs reveals variation of intensity for several peaks at wavelength numbers 1200 cm^{-1}, 1580 cm^{-1}, and 3420 cm^{-1}, along with the reduction in PAC size. In accordance with a previous study, the regions between 1320 and 1050 cm^{-1}, 1610 - 1550 cm^{-1} and 3570 - 3200 cm^{-1} are attributed to the C–O stretch, carboxylate (COO^-) and OH stretching vibration, respectively (Coates, 2000). This may suggest an increase in oxygen-containing functional groups on activated carbon surface during the wet ball milling process, which would shift the point of pH_{PZC} due to acid-base reaction on the surface (Stumm and Schindler, 1987). Takaesu and coworkers have suggested that during the ball milling process, PAC undergoes a reaction with hydroxide ions in the surrounding water, leading to an increase in the oxygen content within the functional groups on the surface of PAC (Takaesu et al., 2019).

3.2. Adsorption performance of PAC and BPAC for target pesticides

To compare the adsorption kinetics, isotherms and thermodynamic of PAC-38, PAC-25, PAC-12, PAC-6, and PAC-1, adsorption experiments were conducted for six pesticides with diverse hydrophobicity (expressed as log*K*ow, Table 2) in surface water samples.

3.2.1. Adsorption kinetics

The adsorption kinetics for the six pesticides versus reaction time (for the initial 60 min) are illustrated in Fig. 1. At the PAC dosages of 10 mg/L, PAC with small sizes (e.g., PAC-1, PAC-6) showed significantly high removal efficiencies. As can be seen from Table S3, in the case of the pesticides with a higher hydrophobic property, such as diazinon and fenitrothion (log*K*ow > 3.3), the reaction rate k^* of PAC-1 increases twenty-fold, compared to that of the commercial PAC-38. This may indicate that, although the BET specific surface areas do not increase upon the milling process, the 'effective' adsorption surface of the PAC should have greatly increased. Note that, the BET specific surface areas with nitrogen gas adsorption reflect both external surface and internal pore surface of the PAC particles. While nitrogen gas could penetrate into the nano-scale pores of PAC, the diffusion of organic compounds into these pores could be an extremely slow process (Matsui et al., 2015). It was suggested that, reducing the particle diameter may not only increase the external surface area but also shortens the internal diffusion pathway of PAC, thus improving diffusion of adsorbate molecules to internal pores and increasing the adsorption kinetics (Partlan et al., 2020; Nakayama et al., 2020). This is probably true, but very much likely in a much less significant level. Considering the great magnitudes of the increase in the external surface of the PAC particles from 38 to 1 μm, corresponding to over a 1000-fold increase, the great magnitude increase of the external surface should be the dominant factor for the increase of adsorption rate kinetics observed in the experiments. Therefore, most likely, the diffusional adsorption from the bulk solution to the external adsorption of the PAC particles may be the dominant adsorption mechanisms.

Besides, compared to hydrophobic pesticides, the hydrophilic pesticide dimethoate (log*K*ow = 0.78), the value of k^* showed only a slight increase from 0.13 min^{-1} to 0.14 min^{-1} as the particle size of PAC decreased. This may indicate that transportation of the hydrophilic molecular adsorbates onto the particle surface was jeopardized at the vicinity of the particle surface. It seems that more activation energy would be required for the hydrophilic molecules to absorb at the water-solid interface due to their strong affinity with the water molecule in solution. Thus, reducing the particle size does not significantly improve the adsorption rate for the hydrophilic pesticide.

3.2.2. Equilibrium adsorption isotherms

Both PAC and BPACs demonstrate well-fitted Langmuir isotherms ($r^2 > 0.966$, Table S4) for the adsorption of the target pesticides. This may indicate that the adsorption process onto PAC could be characterized as monolayer adsorption on a homogeneous solid surface (Saadi et al., 2015). As can be seen from Table 2, for a specific PAC, the Langmuir isotherm constant (K_L) exhibited greater values for pesticides with higher log*K*ow, indicating a stronger binding energy or affinity for the hydrophobic molecules (Gadipelli et al., 2019). However, the particle size of BPAC was found to have little significant effects statistically on the values of K_L ($p > 0.05$, see Table S5). This may indicate that milling PAC particles has little effect on the binding energy between PAC and pesticides. Moreover, only a slight change in q_{max} is evident with decreasing particle size of PAC. Take diazinon as an example, q_{max} values ranged from 2.75 μg/mg to 3.04 μg/mg for the PACs with different particle sizes (Table 2). Statistical analysis shows that there is no relationship between the particle size of PAC and q_{max} ($p > 0.05$, see Table S5). This suggests that the maximum pesticide adsorption capacities of PAC be independent of particle size. These findings are in line with previous studies on the adsorption of organic micropollutants by superfine PAC, where the similar results were suggested to be attributed to the non-significant alteration in pore volume of PAC after ball milling (Pan et al., 2017; Wang et al., 2023). However, it should be pointed that

Table 2
log*K*ow values of pesticides and Langmuir isotherm model parameters (K_L (L/μg), q_{max} (μg/mg)) of PACs with varying diameters.

Name	log*K*ow	PAC-38		PAC-25		PAC-12		PAC-6		PAC-1	
		K_L	q_{max}	K_L	q_{max}	K_L	q_{max}	K_L	q_{max}	K_L	q_{max}
Dimethoate	0.78	0.23	1.11	0.30	1.01	0.46	0.81	0.33	0.95	0.25	1.02
Atrazine	2.61	0.72	1.43	1.34	1.24	1.58	1.28	0.98	1.38	1.38	1.25
Isoproturon	2.87	1.52	1.59	2.43	1.44	3.46	1.35	2.72	1.39	2.19	1.52
Thiometon	3.15	1.49	1.88	2.92	1.76	3.95	1.67	3.44	1.63	3.06	1.78
Fenitrothion	3.30	1.70	2.64	3.00	2.59	3.14	2.66	3.33	2.66	4.29	2.46
Diazinon	3.81	2.56	3.04	9.99	2.86	10.25	2.75	8.69	2.87	8.67	3.00

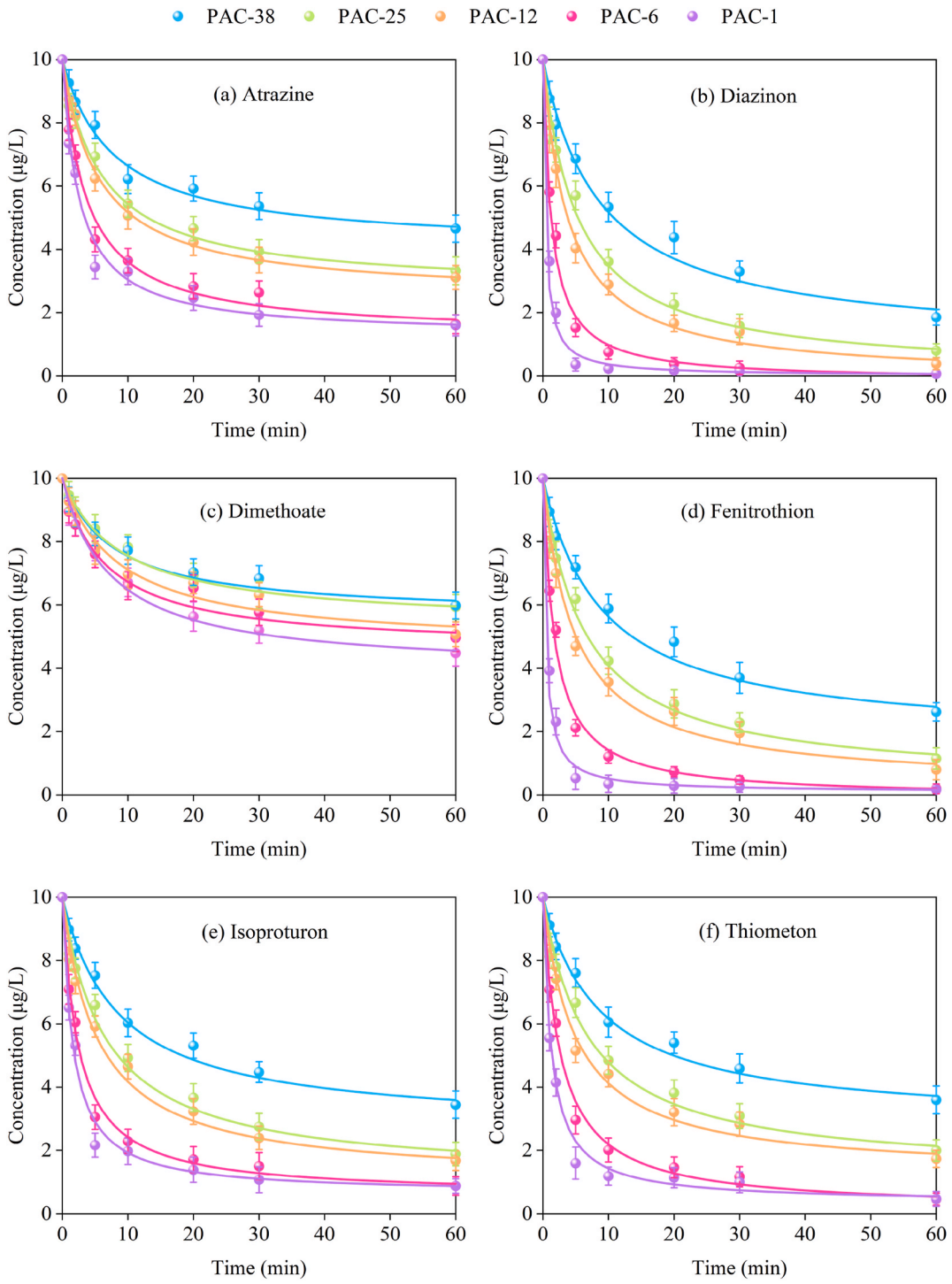

Fig. 1. The adsorption kinetics of six pesticides: (a) atrazine; (b) diazinon; (c) dimethoate; (d) fenitrothion; (e) isoproturon and (f) thiometon onto parent PAC-38 and ball-milled PACs (PAC-25, PAC-12, PAC-6, and PAC-1) at a dosage of 10 mg/L.

the q_{max} values were calculated based on the adsorbate concentrations at equilibrium adsorption (12 h in this study). It does not reflect the adsorption loading of the pesticides within the short retention reaction time (i.e, 1 h).

Between different pesticide types, q_{max} values increased with the log*K*ow values. Take PAC-38 as an example, the maximum pesticide adsorption capacities for dimethoate, atrazine, isoproturon, thiometon, fenitrothion and diazinon were 1.11, 1.43, 1.59, 1.88, 2.64 and 3.04 μg/mg, respectively (see Table 2). This is consistent with some previous studies, suggesting that pollutants with higher log*K*ow values exhibit a greater adsorption affinity towards PAC (Campinas et al., 2021; Jamil et al., 2019). This phenomenon is attributed to the hydrophobic nature of PAC, which preferentially absorbs hydrophobic pesticides due to the hydrophobic interactions or attractions at the solid-liquid interface (Campinas et al., 2021; Li et al., 2016).

3.2.3. *Adsorption thermodynamic*

From the principles of thermal dynamics, a positive ΔG° indicates the need for external drive energy during the adsorption process, while a negative ΔG° suggests a spontaneous adsorption (Saha and Chowdhury,

2011). The negative standard adsorption ΔG° values for all the six pesticides obtained in this study (see Table S6) support that the adsorption process between the pesticides and PAC occurs spontaneously. Additionally, as observed in Table S6, the ΔH° values for all six pesticides were negative, signifying that the adsorption processes between PAC and pesticides were exothermic (Saha and Chowdhury, 2011). Specifically, the ΔH° values for atrazine, diazinon, fenitrothion, isoproturon and thiometon ranging from −18.26 to −41.78 kJ/mol fall within the typical range of 0 to −42 kJ/mol for physical adsorption (Wang et al., 2007), likely suggesting a nature of physical adsorption for these compounds. Conversely, the adsorption of dimethoate (ΔH° = −50.76 kJ/mol) by PAC may exhibit characteristics of chemical adsorption (typical values of ΔH°: −42 to −125 kJ/mol) (Wang et al., 2007).

For entropy change (ΔS°), a positive value suggests increased randomness at the solid/solution interface with some structural changes in the adsorbate and the adsorbent, while a negative value implies a decreased disorder at the solid/liquid interface during the adsorption process (Saha P and Chowdhury S, 2011). Nevertheless, ΔS° may also reflect generally the relative randomness of adsorbate in the whole adsorption system before and after adsorption. This may be probably true in a large part, particularly when considering the thermodynamic parameters are calculated from adsorbate concentrations. As shown in Table S6, the values of ΔS° for diazinon, fenitrothion, and thiometon with higher degree of hydrophobicity are positive, 71.42, 49.27 and 21.57 J/(mol K), respectively. This indicates that these hydrophobic adsorbates acquired more randomness during adsorption, possibly because they were initially associated to some extent in solution due to their hydrophobic interactions with the polar solvent. Conversely, negative ΔS° values were obtained for isoproturon, atrazine and dimethoate with a relative degree of hydrophilicity. This implies a decreased disorder of the adsorbates during the adsorption process in the adsorption system (Saha P and Chowdhury S, 2011). This may indicate that, being hydrophilic, these molecules would have been more dispersed evenly in water solution, so having more randomness in solution than that after they have adsorbed on the particle surfaces. From thermal dynamic adsorption equation (Eq. 8), the adsorption process of the pesticides with less hydrophobic is an enthalpy driven process.

3.3. The residual turbidity and particle numbers after conventional CSF treatment

As shown in Fig. 2, the addition of PACs increased the turbidity of the raw water. Specifically, adding 10 mg/L of commercial PAC-38 resulted in a slight rise in turbidity from 3.3 NTU to 4.6 NTU. However, when PAC-25, PAC-12, PAC-6, and PAC-1 were added, at the same mass concentration of 10 mg/L, the turbidity of the raw water increased to 6.7 NTU, 12.8 NTU, 20.8 NTU, and 52.1 NTU, respectively. Photographic evidence of the raw water samples spiked with the different particle sizes of PAC further confirmed the observed increase in turbidity (Fig. S5). Following coagulation/flocculation and sedimentation, the turbidity of clarified water decreased significantly. Take PAC-1 as an example, the residual turbidity of clarified water is 7.9 NTU, which is notably lower than the initial value of 52.1 NTU for the raw water. The unsettled particles would be effectively removed by the quartz sand filtration, and the turbidity of filtered water was measured to less than 0.2 NTU for all PACs (Fig. 2).

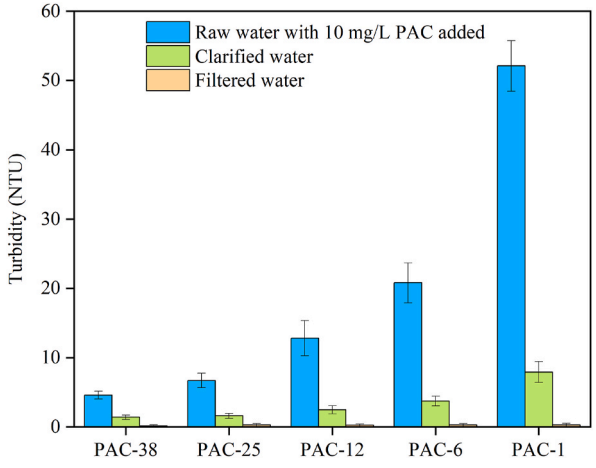

Fig. 2. The turbidity in raw water with the addition of 10 mg/L PAC-38, PAC-25, PAC-12, PAC-6 and PAC-1, the clarified water after coagulation/flocculation and sedimentation treatment, as well as the filtered water after CSF treatment.

Nevertheless, analysis of microscopic images from 0.2 μm filter membranes, after passing through 100 mL of filtered water by the granular filtration, revealed the presence of residual PAC particles (Fig. 3). This indicates that a small amount of very fine PAC particles penetrated through the sand media filter. The amounts of the escaped fine particles varied according to PAC sizes. To estimate the residual PAC number concentrations in the filtrate from sand filtration (N_{PAC}, particles/mL), Eq. (8) was employed,

$$N_{PAC} = \frac{n_{Ave} \times F}{V} \quad (8)$$

where n_{Ave} (particles/mm^2) represents the average number of PAC particles per unit area, calculated based on observations from nine microscope fields of view (FOV) (see Fig. S3). F (mm^2) is the effective filter area of the membrane, and V (mL) is the filtrate volume passing through the membrane.

In this study, the dimensions of the rectangular FOV are 0.0713 mm^2 (length: 310 μm, width: 230 μm), the value of F (circle, radius: 19 mm) and V are 1133.54 mm^2 and 100 mL, respectively. For PAC particle size greater than or equal 5.8 μm, the values of n_{Ave} ranged from 25.2 to 33.7 particles/mm^2; while for PAC-1, the value of n_{Ave} is 162.7 particles/mm^2, which is significantly higher than those observed for other PACs with larger sizes. According to Eq. (8), N_{PAC} can be calculated, and the N_{PAC} values for both PAC and BPACs are listed in Table S7. The N_{PAC} in the sand filtrate were 286–382 particles/mL for PAC-38, PAC-25, PAC-12 and PAC-6, whereas the N_{PAC} for PAC-1 was up to 1844 particles/mL. The above PAC number concentrations in the sand filtrate were comparable to those in a previous study (Nakazawa et al., 2018), and the results confirmed that very fine PAC (e.g., PAC-1) were less efficiently removed by CSF and tended to pass through the sand filter. The passing through of the large numbers of the PAC particles adsorbed with toxic pesticides in the filtrate may pose a harmful effect on human health. Therefore, PAC-6 was chosen for further experiments due to its more removable characteristics compared to PAC-1 and a faster adsorption rate and final removal efficiency for pesticides than other PACs.

3.4. Examination with conventional CSF treatment coupled with PAC-6 for pesticide removal

The removal efficiencies of the six pesticides through CSF treatment with/without the commercial PAC-38 and ball-milled PAC-6 were compared. As shown in Fig. 4, an increase in PAC dosage led to a gradual decrease in the residual concentrations of these pesticides. In the absence of PAC, the removal efficiencies for these pesticides were only range from 1.7% to 13.2%, indicating that conventional CSF treatment alone was not adequate for removing these pesticides. This observation is in line with the previous studies, in which the removal efficiencies for most of the organic micropollutants through conventional CSF treatment were often limited, except for those with very high hydrophobicity (Alexander et al., 2012; Li et al., 2016).

With the addition of PAC, removal efficiency of these pesticides increased greatly. For example, the removal efficiency of diazinon

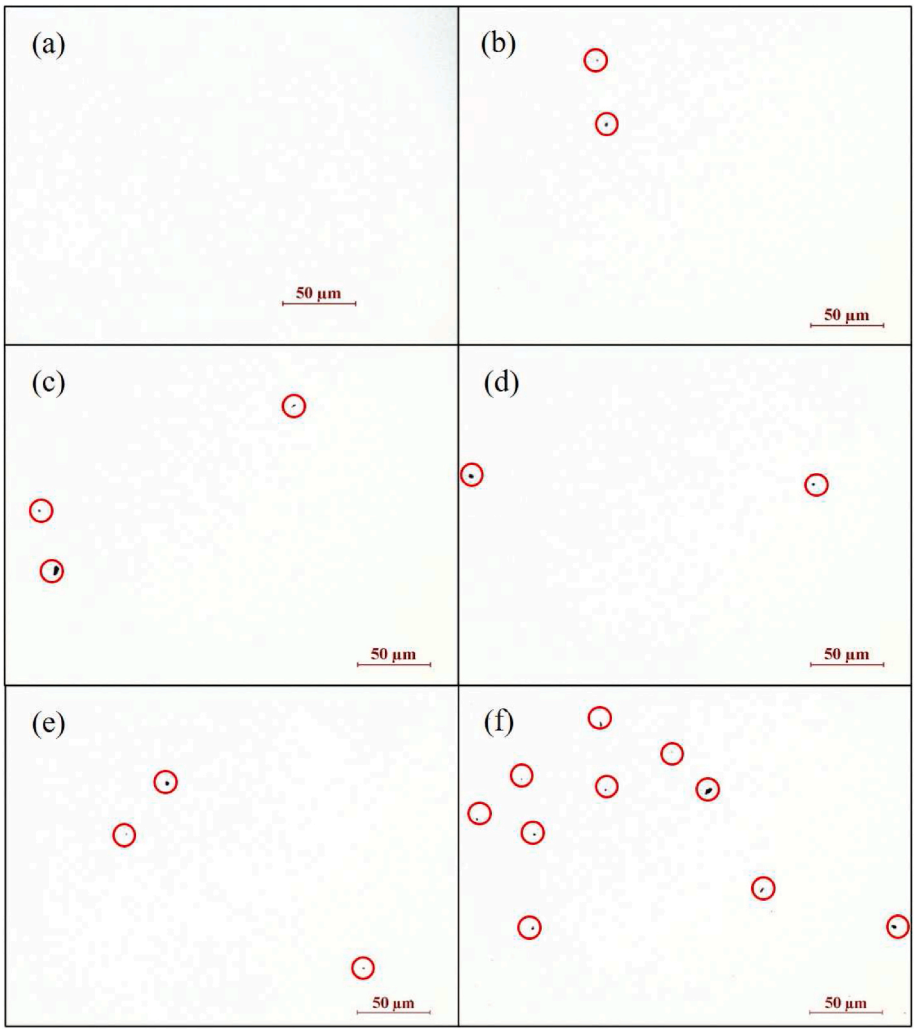

Fig. 3. Microscopic images of PAC and BPACs residues in filtrate: (a) without PAC addition; (b) PAC-38; (c) PAC-25; (d) PAC-12; (e) PAC-6; (f) PAC-1.

gradually increased from 13.2% to 86.0% with the addition of commercial PAC-38 from 0 to 30 mg/L, but further increasing the PAC-38 dosage only obtained a slight increase in the removal efficiency (Fig. 4 (b)). In comparison, when PAC-6 was applied, the removal efficiency of all the pesticides increased significantly compared to those of PAC-38 with the addition of the same PAC dosage. Take the atrazine as an example, adding 60 mg/L of commercial PAC-38 the concentration of atrazine decreased from the initial 10 μg/L to the guideline value of 2 μg/L (SAMR, 2022). In comparison, using 15 mg/L of PAC-6 could achieve the similar removal efficiency while saving approximately 75% in activated carbon dosage (Fig. 4(a)). For the other pesticides, using PAC-6 instead of commercial PAC-38 could reduce the PAC dosage up to 50%–75% for diazinon, fenitrothion, isoproturon, thiometon, and 25% for dimethoate. More importantly, this reduced the initial concentration from 10 μg/L to very low levels to meet the drinking water guidelines (4 μg/L for diazinon (NHMRC, 2011), 6 μg/L for dimethoate (WHO, 2011; SAMR, 2022), 7 μg/L for fenitrothion (NHMRC, 2011), 9 μg/L for isoproturon (WHO, 2011), and 4 μg/L for thiometon (NHMRC, 2011)). As detailed in section 3.2, the higher adsorption rate of PAC-6 for pesticides compared to PAC-38 allows it to adsorb quickly the pesticides within the limited retention time.

The removal efficiencies of these pesticides by PAC-6 assisted CSF treatment were further evaluated under four raw source water quality conditions. The four surface water samples collected from the Feng River, the Wei River, the Shibianyu Reservoir and Hancheng Lake were selected for examinations. All of water samples were spiked with 10 μg/L of atrazine, diazinon, dimethoate, fenitrothion, isoproturon and thiometon for testing purpose. The experimental results demonstrated that the water matrices have certain impacts on the removal of pesticides depending on the source water qualities. As shown in Table 3, with the addition of PAC-38 and PAC-6, removal efficiencies of hydrophobic pesticides (log*K*ow > 3.0) such as diazinon, fenitrothion and thiometon remained consistently comparable for the different raw water qualities, while those of atrazine, dimethoate and isoproturon slightly decreased. It has been reported that hydrophobic pesticides could bind with organic matter polyelectrolytes through hydrogen bonding, pi bonding, and hydrophobic interactions, thus subsequently be effectively removed through processes like PAC adsorption and/or CSF treatment (Alexander et al., 2012; Li et al., 2018). Therefore, with an increase in NOM, although the organic matter in raw water may compete for adsorption sites on PAC, the removal efficiencies of these pesticides exhibit slight variations due to the additional removal mechanisms. In the case of less hydrophobic organic pesticides, the observed decrease in removal efficiencies could be attributed to the competitive adsorption between pesticides and organic matter fractions (Campinas et al., 2021). Nevertheless, the addition of 15 mg/L PAC-6 proved effective in achieving residual concentrations of target pesticides below the drinking water quality guidelines for all the studied raw waters, much lower than the dosage required for commercial PAC-38 (up to 70 mg/L). These results indicate that application of BPAC with sample particle sizes like the PAC-6 could achieve high rate adsorption of the pesticides, thus high removal efficiency and potential saving of activated carbon dosage for

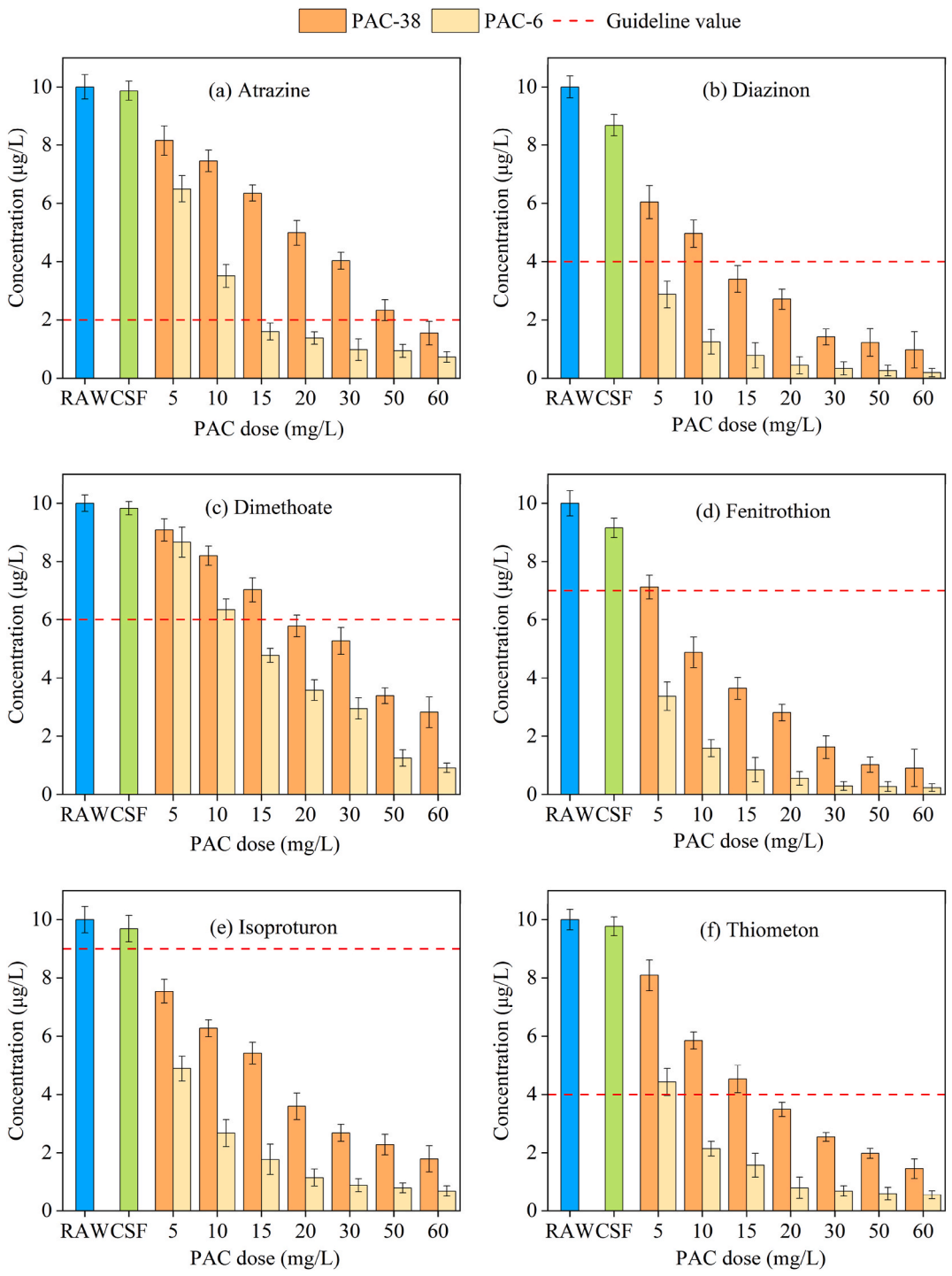

Fig. 4. Residual concentration of (a) atrazine (guideline value (GV) of China: 2 μg/L); (b) diazinon (GV of Australia: 4 μg/L); (c) dimethoate (GV of China and WHO: 6 μg/L); (d) fenitrothion (GV of Australia: 7 μg/L); (e) isoproturon (GV of WHO: 9 μg/L) and (f) thiometon (GV of Australia: 4 μg/L) treated by PAC-38 and PAC-6 at various dosages in a conventional CSF treatment process.

different water qualities.

4. Conclusions

This study investigated the removal efficiencies of six pesticides (atrazine, diazinon, dimethoate, fenitrothion, isoproturon and thiometon) using PACs with varying particle sizes in a conventional CSF for drinking water treatment. Despite minimal changes in the maximum adsorption capacity of PAC, the adsorption rate of pesticides significantly increased with decreasing particle size. PAC-1 exhibited the highest adsorption rate for all target pesticides; however, its effective removal through conventional CSF treatment proved challenging, leading to a much higher concentration of PAC particles in the sand filtrate compared to other PACs. To address this, PAC-6 emerged as the optimal choice, simultaneously achieving high removal efficiencies of pesticides and low residual PAC particles. In pursuit of meeting drinking water guideline values, the application of PAC-6 in the conventional CSF treatment system demonstrated the potential for significant PAC dosage savings, reaching up to 75% when compared to commercial PAC-38. Notably, water matrices had minimal effects on hydrophobic

Table 3
Removal of pesticides from five source waters by 60 mg/L PAC-38 and 15 mg/L PAC-6.

Source water		Removal efficiencies (%)					
		Atrazine	Diazinon	Dimethoate	Fenitrothion	Isoproturon	Thiometon
Jinpen Reservoir	PAC-38	84.6 ± 4.1	90.3 ± 6.2	71.8 ± 5.3	90.9 ± 6.4	82.1 ± 4.5	85.5 ± 3.4
	PAC-6	84.1 ± 2.9	92.2 ± 4.3	52.2 ± 2.4	91.5 ± 4.2	82.3 ± 5.2	84.3 ± 4.1
Feng River	PAC-38	83.1 ± 4.4	89.6 ± 4.3	67.3 ± 4.6	89.3 ± 6.4	83.6 ± 5.5	85.9 ± 6.5
	PAC-6	84.7 ± 3.4	91.0 ± 4.2	50.3 ± 5.7	90.2 ± 6.3	81.8 ± 6.3	84.1 ± 4.7
Wei River	PAC-38	79.3 ± 4.2*	89.9 ± 2.4	63.9 ± 5.5	88.7 ± 4.4	77.3 ± 2.4	82.5 ± 5.2
	PAC-6	84.2 ± 3.5	90.7 ± 5.2	49.1 ± 3.9	90.8 ± 5.5	78.2 ± 4.3	82.0 ± 2.5
Shibianyu Reservoir	PAC-38	76.3 ± 4.8*	86.6 ± 3.9	59.3 ± 5.9	86.3 ± 2.7	73.2 ± 5.1	79.1 ± 6.1
	PAC-6	82.6 ± 3.7	87.5 ± 4.0	47.5 ± 4.3	86.1 ± 3.4	76.3 ± 4.2	80.7 ± 5.5
Hancheng Lake	PAC-38	75.4 ± 4.3*	84.2 ± 6.7	60.6 ± 5.9	83.5 ± 6.0	72.6 ± 4.7	75.9 ± 4.7
	PAC-6	81.5 ± 3.6	85.9 ± 5.8	51.4 ± 5.4	84.9 ± 6.1	75.5 ± 6.3	77.2 ± 6.2

Note: *To achieve to the guideline values 2 μg/L, a dosage of 70 mg/L PAC-38 is required.

pesticides (e.g., diazinon, fenitrothion, and thiometon) but showed slight negative impacts on less hydrophobic pesticides (e.g., atrazine, dimethoate and isoproturon). The addition of 15 mg/L PAC-6 successfully resulted in residual concentrations of target pesticides below drinking water quality guidelines for all studied raw waters. These findings demonstrated the feasibility and cost-effectiveness of employing PAC-6 for removing various pesticides in the conventional drinking water treatment process.

CRediT authorship contribution statement

Wei Li: Writing – original draft, Supervision, Funding acquisition. **Congjian Dong:** Validation. **Zijing Hao:** Validation. **Xinyi Wu:** Formal analysis. **Donghai Ding:** Resources. **Jinming Duan:** Writing – review & editing.

Declaration of competing interest

The authors declare that they have no known competing financial interests or personal relationships that could have appeared to influence the work reported in this paper.

Data availability

Data will be made available on request.

Acknowledgements

The authors wish to express their thanks for the financial support from the Natural Science Foundation of Shaanxi Province (Grant No. 2024JC-YBMS-229), the Shaanxi Provincial Key Scientific and Technological Innovation Team (2023-CX-TD-32) and the China ScholarshipFoundation (Grant No. LJM-2023-25).

Appendix A. Supplementary data

Supplementary data to this article can be found online at https://doi.org/10.1016/j.chemosphere.2024.142229.

References

Ahmed, S., Mofijur, M., Nuzhat, S., Chowdhury, A.T., Rafa, N., Uddin, M.A., Inayat, A., Mahlia, T., Ong, H.C., Chia, W.Y., 2021. Recent developments in physical, biological, chemical, and hybrid treatment techniques for removing emerging contaminants from wastewater. J. Hazard Mater. 416, 125912.
Al-Asad, H.A., Parniske, J., Qian, J., Alex, J., Ramaswami, S., Kaetzl, K., Morck, T., 2022. Development and application of a predictive model for advanced wastewater treatment by adsorption onto powdered activated carbon. Water Res. 217, 118427.
Alexander, J.T., Hai, F.I., Al-Aboud, T.M., 2012. Chemical coagulation-based processes for trace organic contaminant removal: current state and future potential. J. Environ. Manag. 111, 195–207.
Bonvin, F., Jost, L., Randin, L., Bonvin, E., Kohn, T., 2016. Super-fine powdered activated carbon (SPAC) for efficient removal of micropollutants from wastewater treatment plant effluent. Water Res. 90, 90–99.
Brovini, E.M., Moreira, F.D., Martucci, M.E.P., de Aquino, S.F., 2023. Water treatment technologies for removing priority pesticides. J. Water Process Eng. 53, 103730.
Campinas, M., Silva, C., Viegas, R.M., Coelho, R., Lucas, H., Rosa, M.J., 2021. To what extent may pharmaceuticals and pesticides be removed by PAC conventional addition to low-turbidity surface waters and what are the potential bottlenecks? J. Water Process Eng. 40, 101833.
Coates, J., 2000. Interpretation of infrared spectra, A practical approach. In: Encyclopedia of Analytical Chemistry. John Wiley & Sons Ltd, Chichester, 2000.
de Souza, R.M., Seibert, D., Quesada, H.B., de Jesus Bassetti, F., Fagundes-Klen, M.R., Bergamasco, R., 2020. Occurrence, impacts and general aspects of pesticides in surface water: a review. Process Saf. Environ. Prot. 135, 22–37.
Desisa, B., Getahun, A., Muleta, D., 2022. Advances in biological treatment technologies for some emerging pesticides. In: Pesticides Bioremediation. Springer.
Gadipelli, B. Wood, Ramisetty, K.K., Stewart, A.A., Howard, C.A., Brett, D., Rodriguez-Reinoso, F., 2019. Characterization of adsorption site energies and heterogeneous surfaces of porous materials. J. Mater. Chem. A 7, 10104–10137.
Ghosal, P.S., Gupta, A.K., 2017. Determination of thermodynamic parameters from Langmuir isotherm constant-revisited. J. Molecular Liquids 225, 137–146.
Gilliom, R.J., 2007. Pesticides in US Streams and Groundwater. ACS Publications.
Ho, Y.S., McKay, G., 1999. Pseudo-second order model for sorption processes. Process Biochem. 34 (5), 451–465.
Jamil, S., Loganathan, P., Listowski, A., Kandasamy, J., Khourshed, C., Vigneswaran, S., 2019. Simultaneous removal of natural organic matter and micro-organic pollutants from reverse osmosis concentrate using granular activated carbon. Water Res. 155, 106–114.
Khan, S.U., 2016. Pesticides in the Soil Environment. Elsevier.
Li, W., Liang, X., Duan, J., Beecham, S., Mulcahy, D., 2018. Influence of spent filter backwash water recycling on pesticide removal in a conventional drinking water treatment process. Environ. Sci.: Water Res. Technol. 4 (7), 1057–1067.
Li, W., Liu, Y., Duan, J., Saint, C.P., Mulcahy, D., 2015. The role of methanol addition to water samples in reducing analyte adsorption and matrix effects in liquid chromatography–tandem mass spectrometry. J. Chromatogr., A 1389, 76–84.
Li, W., Wu, R., Duan, J., Saint, C.P., van Leeuwen, J., 2016. Impact of prechlorination on organophosphorus pesticides during drinking water treatment: removal and transformation to toxic oxon byproducts. Water Res. 105, 1–10.
Li, W., Zhao, Y., Yan, X., Duan, J., Saint, C.P., Beecham, S., 2019. Transformation pathway and toxicity assessment of malathion in aqueous solution during UV photolysis and photocatalysis. Chemosphere 234, 204–214.
Matsui, Y., Nakao, S., Sakamoto, A., Taniguchi, T., Pan, L., Matsushita, T., Shirasaki, N., 2015. Adsorption capacities of activated carbons for geosmin and 2-methylisoborneol vary with activated carbon particle size: effects of adsorbent and adsorbate characteristics. Water Res. 85, 95–102.
Matsushita, T., Morimoto, A., Kuriyama, T., Matsumoto, E., Matsui, Y., Shirasaki, N., Kondo, T., Takanashi, H., Kameya, T., 2018. Removals of pesticides and pesticide transformation products during drinking water treatment processes and their impact on mutagen formation potential after chlorination. Water Res. 138, 67–76.
Meffe, R., de Bustamante, I., 2014. Emerging organic contaminants in surface water and groundwater: a first overview of the situation in Italy. Sci. Total Environ. 481, 280–295.
Meftaul, I.M., Venkateswarlu, K., Dharmarajan, R., Annamalai, P., Megharaj, M., 2020. Pesticides in the urban environment: a potential threat that knocks at the door. Sci. Total Environ. 711, 134612.
Mostafalou, S., Abdollahi, M., 2017. Pesticides: an update of human exposure and toxicity. Arch. Toxicol. 91 (2), 549–599.
Müller, G., Radke, C., Prausnitz, J., 1985. Adsorption of weak organic electrolytes from dilute aqueous solution onto activated carbon. Part I. Single-solute systems. J. Colloid Interface Sci. 103 (2), 466–483.
Najm, I.N., 1996. Mathematical modeling of PAC adsorption processes. J. - Am. Water Works Assoc. 88 (10), 79–89.
Nakayama, A., Sakamoto, A., Matsushita, T., Matsui, Y., Shirasaki, N., 2020. Effects of pre, post, and simultaneous loading of natural organic matter on 2-methylisoborneol adsorption on superfine powdered activated carbon: reversibility and external pore-blocking. Water Res. 182, 115992.

Nakazawa, Y., Matsui, Y., Hanamura, Y., Shinno, K., Shirasaki, N., Matsushita, T., 2018. Identifying, counting, and characterizing superfine activated-carbon particles remaining after coagulation, sedimentation, and sand filtration. Water Res. 138, 160–168.
Naughton, S.X., Terry Jr, A.V., 2018. Neurotoxicity in acute and repeated organophosphate exposure. Toxicology 408, 101–112.
NHMRC, 2011. Australian Drinking Water Guidelines. National Health and Medical Research Council (NHMRC).
Nicolopoulou-Stamati, P., Maipas, S., Kotampasi, C., Stamatis, P., Hens, L., 2016. Chemical pesticides and human health: the urgent need for a new concept in agriculture. Front. Public Health 4, 148.
Pan, L., Nishimura, Y., Takaesu, H., Matsui, Y., Matsushita, T., Shirasaki, N., 2017. Effects of decreasing activated carbon particle diameter from 30 μm to 140 nm on equilibrium adsorption capacity. Water Res. 124, 425–434.
Partlan, E., Ren, Y., Apul, O.G., Ladner, D.A., Karanfil, T., 2020. Adsorption kinetics of synthetic organic contaminants onto superfine powdered activated carbon. Chemosphere 253, 126628.
Pimentel, D., 1995. Amounts of pesticides reaching target pests: environmental impacts and ethics. J. Agric. Environ. Ethics 8, 17–29.
Richardson, J.R., Fitsanakis, V., Westerink, R.H., Kanthasamy, A.G., 2019. Neurotoxicity of pesticides. Acta Neuropathol. 138, 343–362.
Saadi, R., Saadi, Z., Fazaeli, R., Fard, N.E., 2015. Monolayer and multilayer adsorption isotherm models for sorption from aqueous media. Kor. J. Chem. Eng. 32, 787–799.
Saha, P., Chowdhury, S., 2011. Insight into adsorption thermodynamics. Thermodynamics 16, 349–364.
SAMR, 2022. Standards for Drinking Water Quality. State Administration for Market Regulation (SAMR). of China.
Simonin, J.P., 2016. On the comparison of pseudo-first order and pseudo-second order rate laws in the modeling of adsorption kinetics. Chem. Eng. J. 300, 254–263.
Siri, C., Liu, Y., Masset, T., Dudefoi, W., Oldham, D., Minghetti, M., Grandjeana, D., Breider, F., 2021. Adsorption of progesterone onto microplastics and its desorption in simulated gastric and intestinal fluids. Environ. Sci.: Process. Impacts 23 (10), 1566–1577.
Statista Research Department, 2023. Agricultural consumption of pesticides worldwide from 1990 to 2021. https://www.statista.com/statistics/1263077/global-pesticide-agricultural-use/.
Stumm, W.A., Schindler, P.W., 1987. Aquatic surface chemistry: chemical processes at the particle-water interface. In: Stumm, W. (Ed.), The Surface Chemistry of Oxides, Hydroxides, and Oxide Minerals. John Wiley and Sons, New York, USA.
Takaesu, H., Matsui, Y., Nishimura, Y., Matsushita, T., Shirasaki, N., 2019. Micro-milling super-fine powdered activated carbon decreases adsorption capacity by introducing oxygen/hydrogen-containing functional groups on carbon surface from water. Water Res. 155, 66–75.
Tran, H.N., You, S.J., Hosseini-Bandegharaei, A., Chao, H.P., 2017. Mistakes and inconsistencies regarding adsorption of contaminants from aqueous solutions: a critical review. Water Res. 120, 88–116.
Tudi, M., Daniel Ruan, H., Wang, L., Lyu, J., Sadler, R., Connell, D., Chu, C., Phung, D.T., 2021. Agriculture development, pesticide application and its impact on the environment. Int. J. Environ. Res. Public Health. 18 (3), 1112.
Wang, J.P., Feng, H.-M., Yu, H.-Q., 2007. Analysis of adsorption characteristics of 2, 4-dichlorophenol from aqueous solutions by activated carbon fiber. J. Hazard Mater. 144 (1–2), 200–207.
Wang, Y., Zhang, Z., Yin, Z., Wang, J., Zhang, X., Chen, C., 2023. Adsorption of typical NDMA precursors by superfine powdered actived carbon: critical role of particle size reduction. J. Environ. Sci. 147, 101–113.
WHO, 2011. Guidelines for Drinking-Water Quality. World Health Organization (WHO), fourth ed.
Wu, F.C., Tseng, R.L., Huang, S.C., Juang, R.S., 2009. Characteristics of pseudo-second-order kinetic model for liquid-phase adsorption: a mini-review. Chem. Eng. J. 151 (1–3), 1–9.
Zhang, Y., Zhao, J., Liu, Z., Tian, F., Lu, J., Mu, R., 2021. Coagulation removal of microplastics from wastewater by magnetic magnesium hydroxide and PAM. J. Water Process Eng. 43, 102250.